Polyaniline as a Sacrificing Template for the Synthesis of Ultra-small Co3O4 Nanoparticles for the Sensitive and Selective Detection of Methotrexate (MTX)

Irum Naz Qureshi
University of Sindh
Aneela Tahira
University of Sindh
Khoulwod Aljadoa
King Saud University
Ali M. Alsalme
King Saud University
Asma A. Al-Othman
King Saud University
Ayman Nafady
King Saud University
Amal Kasry
The British University in Egypt
Zafar Hussain Ibupoto (zaffar.ibhupoto@usindh.edu.pkk)
University of Sindh https://orcid.org/0000-0002-6756-9862

Research Article

Keywords: Polyaniline, Co3O4 nanoparticles, hydrothermal method, methotrexate (MTX), anticancer drug, BRB buffer

Posted Date: February 26th, 2021

DOI: https://doi.org/10.21203/rs.3.rs-248125/v1

Abstract

The successful monitoring of the anticancer drugs using nanostructured materials is very important but very challenging task. Beside this, uniform and ultra-small size of metal oxide nanoparticles is highly needed in order to enhance the catalytic activity which could result into the development of sensitive and selective electrochemical sensors for methotrexate (MTX). For this purpose, we have used a simple approach involving the polyaniline (PANI) as a sacrificing template for the growth of uniform and ultra-small Co_3O_4 nanoparticles by hydrothermal method. The structure, shape, composition and phase purity were studied by scanning electron microscopy (SEM), energy dispersive spectroscopy (EDS), X-ray diffraction (XRD) and Fourier transform Infrared (FTIR) techniques. The average size of Co_3O_4 nanoparticles was below 50 nm. The cubic crystallography is confirmed for the Co_3O_4 nanoparticles. The electrochemical properties of PANI assisted Co_3O_4 nanoparticles for MTX drug was evaluated by cyclic voltammetry (CV) and linear sweep voltammetry (LSV) in Britton–Robinson buffer (BRB) of pH 3.5. The PANI assisted Co_3O_4 nanoparticles were found highly sensitive for the MTX drug and exhibited a linear range from 5-75μM of MTX and limit of detection for the modified electrode was estimated 1.98μM. The proposed electrochemical sensor is low cost, simple, highly sensitive and selective towards MTX detection. The synthetic methodology using the conducting polymer as a sacrificing template for the growth of controlled and ultra-small Co_3O_4 nanoparticles can be utilized for the wide range of electrochemical applications.

1. Introduction

Cancer disease has been remained chronic issue since decades and it causes many deaths annually. The critical handling of this problem resulted the synthesis of several expensive drugs and diagnosis devices. Methotrexate (MTX) is derived from the folic acid antagonist and has been used widely in chemotherapy as a cure for various cancer diseases including leukemia, breast cancer, lung cancer, osteosarcoma, and lymphoma. MTX is also used as cure for the autoimmune diseases like rheumatoid arthritis, psoriasis and Crohn,s illness [1–3]. MTX is also effective for the head and neck cancer. MTX has potential to inhibit the cell development via bonding to dihydrofolate reductase to eliminate the reduction of dihydrofolate to tetrahydrofolate [4]. On other side, MTX has severe side effects like other chemo drugs [5, 6]. It has been found that the MTX value above 10 μM in plasma is highly dangerous for the time of 10 h [7]. The high level of MTX in the blood decreases the development of noncancerous cells and causes heart stroke, liver and poisoning effect to lungs and ulcer of stomach [8]. Hence it is very vital to control on the use of MTX during the chemotherapy and should be monitored by low cost and quick analytical methods with high accuracy in order to improve effectiveness of drug and its safety. In the recent past, the designing a facile, fast, and very sensitive analytical method for the determination of MTX has received considerable attention. Currently, the analytical techniques such as capillary electrophoresis [9, 0], high performance liquid chromatography [10] and fluorescence spectroscopy [11–13] have been found highly accurate for the determination of MTX from biological samples. These standard analytical methods are costly and require multistep for the sample preparation which restricted their clinical applicability. The

electroanalytical methods have more preference due to their excellent sensitivity, selectivity, facile features, inexpensive nature, quick in response and very suitable for on spot detection. For this purpose, various modified electrodes have been fabricated for the electroanalysis of MTX [14–26]. At the present, the scientists and researchers are using variety of compounds in electroanalytical methods and investigating their activity in different conditions such as clinical samples. The use of multiple semiconducting nanostructures for the modification of conducting electrodes has enabled them to quantify biomolecules and drugs sensitively compared to the conventional electrodes [27]. Among the metal oxide nanostructured materials, cobalt oxide (Co_3O_4) with different shapes have been investigated in different electrochemical applications such as batteries, supercapacitors, and electrocatalysis [28]. Due to unique and attractive properties of Co_3O_4 such as high theoretical capacity, catalytic activity, excellent thermal and chemical stability [28]. However, Co_3O_4 nanostructures are experiencing poor electrical conductivity which adversely brings the unfavorable charge transfer kinetics and poor specific capacitance than the expected value. To uplift the electrical conductivity, different effective strategies have been used in producing the Co_3O_4 composites with conducting polymers, metal oxides and carbon [29–32]. The Co_3O_4 composite material offers unique architecture and enhanced electrical conducting for the determination of pharmaceutical products. The polyaniline (PANI) is low cost, conducting polymer and it can be produced into nano size, thus it is among the appealing conducting polymers [33]. The use of nanostructured PANI is increasing in the recent time in the field of electrochemical sensors due to its attractive physical and chemical characteristics compared to its bulk phase. The properties like flexible nature, high porosity, large surface to volume ratio and swift charge transfer kinetics are obvious for the PANI [34, 35]. The significant redox catalytic activity of Co_3O_4 has been exploited for the oxidation of pharmaceutical products [36, 37]. The Co_3O_4 has been used with PANI and its electron transfer properties were enhanced [38]. The nanostructured PANI has been prepared by the different methods [39–42]. The use of PANI as sacrificing agent for the synthesis of controlled, homogenous, and ultra-small Co_3O_4 nanoparticles is rarely investigated. The PANI as a sacrificing template provides the excellent dispersion of Co_3O_4 due to excess of carbon in the prepared sample in water and it also gives a large number of oxygen defects in the composition. Therefore, it fosters the development of sensitive and selective electrochemical sensors for the detection of biomolecules and pharmaceutical products.

In this study, three steps methodology was used to prepare the ultra-small nanoparticles of Co_3O_4 using PANI as sacrificing template. The structure and composition of prepared Co_3O_4 material was studied by SEM, EDS, XRD and FTIR techniques. The Co_3O_4 nanoparticles were used to modify the glassy carbon electrode (GCE) for the electrochemical determination of MTX in BRB buffer of pH 3.5. The modified electrode has sensitively and selectively quantified the MTX drug with a linear range of 5–75μM and limit of detection of 1.98μM. The successful application of modified electrode for the detection of MTX from blood plasma is also reported.

2. Experimental Section

Cobalt chloride hexahydrate (99%), aniline, urea (99%), glucose (99%), sodium chloride (99%), sucrose, phosphoric acid, acetic acid, potassium chloride (99%) and 5% Nafion (E.W. 1100) were of analytical grade and received from Sigma Aldrich Karachi Pakistan. All the solutions were prepared in the deionized water. A 0.01MBRB buffer solution of pH 3.5 was used as supporting electrolyte. The stock solution of MTX was prepared in BRB buffer solution of pH 3.5.

2.2. Growth of ultra-small Co_3O_4 nanoparticles using PANI as sacrificing template

Hydrothermal method was followed for the growth of ultra-small Co_3O_4 nanoparticles using PANI as sacrificing template. First, PANI was prepared by oxidative polymerization of aniline using ammonium sulfate as an oxidizing agent. The purpose of using PANI as sacrificing agent was to control on the morphology and uniformity of Co_3O_4 nanoparticles. Also, the carbon could be added into the ultra-small Co_3O_4 nanoparticles which can improve the dispersion of ultra-small Co_3O_4 nanoparticles in water during the preparation of catalyst slurry. Then 1 g of PANI was used as support for the deposition of cobalt hydroxide nanostructures using (0.1M) equi-molar solution of cobalt chloride hexahydrate and urea. The growth solution was covered with aluminum sheet very tightly. The hydrothermal process was performed at 95 ^oC for 5 h. Then nanostructured material was collected on the ordinary filter paper and left to dry for overnight. Afterwards, the calcination was carried out at 500 ^oC in air for 4 h in order to complete the transformation of hydroxide phase into oxide and to remove the PANI from the surface of ultra-small Co_3O_4 nanoparticles. The pristine Co_3O_4 nanostructures were synthesized by the same method without the use of PANI as a sacrificing agent.

The morphology, composition, and phase purity of synthesized Co_3O_4 were investigated via SEM attached with EDS at 20 kV. The XRD was applied to measure the crystalline features and phase of prepared nanomaterials using measurement conditions of X-ray source from CuKα radiation (λ = 1.5418 Å), 45 kV and 45 mA. The chemical interaction of Co_3O_4 with PANI was also studied by FTIR analysis.

2.3. Electroanalysis of methotrexate (MTX) using ultra-small Co_3O_4 nanoparticles

The suspension of Co_3O_4 nanoparticles was prepared by dispersing 2 mg in 2 mL deionized water and 50μL of 5% Nafion and homogenous suspension was obtained in ultrasonic bath for 1h. Before the modification of GCE, the polishing was used to clean the surface of GCE using silicon paper and alumina paste, followed by washing with deionized water and drying in air at room temperature. Then, 5 μL of the suspension of Co_3O_4 nanoparticles was deposited on the surface of GCE and dried at 50 ^oC in electric oven for 5 minutes. The electrochemical cell system was consisting Co_3O_4 nanoparticles modified GCE as working electrode, silver-silver chloride (Ag/AgCl) as reference electrode and platinum as counter electrode. The BRB buffer of pH 3.5 was used as a supporting electrolyte. The stock solution of desired

concentration of MTX was prepared in BRB buffer solution. The CV curves were measured at 60 mV/s except scan rate study. The LSV was performed at a scan rate of 10 mV/s.

3. Results And Discussion

3.1. Morphology, crystalline structure and composition characterization of Co_3O_4 nanoparticles

The morphology of Co_3O_4 without and with PANI was studied by SEM as shown in Fig. 1. It could be seen that the pristine Co_3O_4 exhibits a heterogeneous nanostructured like elongated nanoparticles and long rods in the structure. The dimension of elongated nanoparticles could be more than 100 nm as shown in Fig. 1a. However, the use of PANI as sacrificing template has controlled the morphology Co_3O_4 with homogeneous distribution and ultra-small nanoparticles of Co_3O_4 were obtained. The average size of ultra-small Co_3O_4 nanoparticles was measured below 50 nm as shown in Fig. 1c. It is clear from this study that the small particle size of Co_3O_4 shows the large surface area and consequently superior electrocatalytic performance towards the oxidation of MTX was observed. The chemical composition of Co_3O_4 without and with PANI was explored by the EDS analysis as shown in Fig. 1b. The Co_3O_4 sample obtained in the presence of PANI as sacrificing template possess less oxygen concentration compared to the pristine Co_3O_4, indicating oxygen vacancies as shown in Fig. 1d. They have shown a dynamic role in the generation of strong electrical signal during the oxidation of MTX in BRB buffer solution of pH 3.5.

Figure 2a shows the diffraction patterns of pristine Co_3O_4 including 111,220,311, 222,400,422,511, 531,533, and 622 at 2theta degree 18.93°, 31.16 °, 36.72 °, 38.42 °, 44.65 °, 55.46 °, 59.14 °, 68.37 °, 77.04 °, and 78.10° respectively. Similarly, the XRD diffraction patterns were measured for the Co_3O_4 sample obtained with PANI as sacrificing template and they were noticed for the crystal planes such as 111, 220,311, 222,400,422,511, 531,533, and 622 at 2theta degree 18.91°, 31.13 °, 36.68 °, 38.38 °, 44.61 °, 55.40 °, 59.08 °, 68.30 °, 76.97 °, and 78.01 ° respectively. All the observed crystallographic patterns are well matched with the reference (card no: 01-080-1542). This indicates that the complete combustion of PANI at 500 °C in air and only leaving behind the diffraction patterns of Co_3O_4. It was also found that the addition of PANI suppressed the crystal planes towards lower angle which might be assigned to steric effect offered by the long chains of PANI on the growth process of Co_3O_4. From XRD analysis, there was not any other phase or impurity present in the PANI assisted Co_3O_4 sample. From SEM and XRD analysis, it is found that the PANI as sacrificing template has suppressed the crystallite size which is further verified by SEM analysis.

Furthermore, the FTIR study was carried out for Co_3O_4 with and without PANI as a sacrificing template as shown in Fig. 2b. The observed bands at 574 and 676 cm^{-1} in the FTIR spectrum are suggesting the typical characteristic features of spinal Co_3O_4 [43, 44]. The FTIR band at 1033 cm^{-1} are assigned to the

stretching mode of C-O and CO_3^{2-} negatively charge species which could be in the sample during the combustion and growth process of Co_3O_4 [45]. The measured band at 1424 cm^{-1} is corresponded to the stretching mode of nitrogen [45]. In the case of PANI with Co_3O_4, the peak at 1662 cm^{-1} is attributed from a minor impurity introduced by the quinoid ring and N-H stretching band of PANI [46, 47, 48 49]. FTIR study reveals that the PANI was completely burnt thus we could not observe any typical FTIR band for PANI. However, a small variation in the band position of Co_3O_3 sample with PANI suggests its role towards the control on the morphology during the growth process of Co_3O_4 [50].

3.2. The electroanalysis of Co_3O_4 nanoparticles towards MTX drug

Figure 3 shows the CV curves of bare GCE, modified GCE with pristine Co_3O_4 and PANI assisted Co_3O_4 at a scan rate of 60 mV/s in the absence and presence of 20μM MTX concentration in BRB buffer solution of pH 3.5. It can be visualized that the bare GCE showed no activity in buffer solution and pristine Co_3O_4 modified GCE has also shown only the change in the current intensity but no obvious redox peaks even in the presence of 20μM MTX. It indicates that neither bare GCE nor pristine Co_3O_4 are the good electrode materials for the oxidation of MTX. However, the PANI assisted Co_3O_4 samples has shown a very slight oxidation peak in the BRB buffer solution and a prominent oxidation peak in 20μM MTX concentration was measured as shown in Fig. 3. The oxidation peak for the MTX was found at 1.02 V versus Ag/AgCl. From this electroanalysis, we see a dynamic role of PANI as a sacrificing template towards the growth process of Co_3O_4 which has not only controlled on the morphology and composition but also has demonstrated well deserving electrochemical properties for the sensing of MTX drug. These findings suggest that the capability of PANI assisted Co_3O_4 nanostructures to determine the MTX in acidic conditions and the surface of metal oxide nanoparticles is associated with the adsorbed hydroxyl groups. These adsorbed hydroxyl groups on the PANI assisted Co_3O_4 nanostructures caused an electrostatic interaction between the PANI assisted Co_3O_4 nanoparticles and carboxylic groups carried by the MTX itself [51, 52]. Therefore, the PANI assisted Co_3O_4 nanostructures have been used for the modification of GCE for all other measurements.

The influence of scan rate on the oxidation peak current was investigated by CV using PANI assisted Co_3O_4 nanostructures in 20μM MTX concentration as shown in Fig. 4a. The oxidation peak current was irreversibly increased with increasing scan rate and revealing an excellent electrochemical properties of the modified GCE. A linear fitting of oxidation peak current versus square root of scan rate is shown in Fig. 4b, which characterized the diffusion controlled kinetics of PANI assisted Co_3O_4 nanostructures towards MTX. To observe the applicability of PANI assisted Co_3O_4 nanostructures for the sensitive detection of MTX, a concentration window was built ranging from 5–75μM and was tested in BRB buffer solution of pH 3.5 using CV curves as shown in Fig. 5a. The CV curves have demonstrated a successive increase in the oxidation peak current with increase in the MTX concentration. A linear plotting was made between the oxidation peak current and MTX concentration for PANI assisted Co_3O_4 nanostructures as

shown in Fig. 5b. This analysis illustrated an acceptable linear range within 5–75μM MTX concentrations. The limit of detection of the PANI assisted Co_3O_4 nanostructures was found 1.98 μM and limit of quantification was estimated 6.6μM which were calculated according to the published work [53].

The LSV was also used to develop a calibration plot of MTX drug using PANI assisted Co_3O_4 nanostructures as shown in Fig. 6a. It can be seen that the oxidation peak current was linearly increased with addition of higher concentration of MTX. A linear plot was constructed between the peak current and various MTX concentrations as shown in Fig. 6b. It indicates a well-established linear range for the PANI assisted Co_3O_4 nanostructures from 20–70μM of MTX. The limit of detection was obtained 1.18μM and limit of quantification was measured 4μM. To evaluate the selectivity of PANI assisted Co_3O_4 nanostructures towards MTX, interference study was carried out in 20μM MTX concentration and the same concentration of potential interfering species was used. The CV curves were measured and the change in the peak current was noticed for each interfering substance and correlated with the peak current of MTX drug. The measured change in the electrical signal is listed in the Table 1 which suggests that the tested interfering substances such as paclitaxel, mitoxantrone, glucose, sucrose, urea and chloride ions has shown negligible effect on the peak current. This demonstrates the significant selectivity of PANI assisted Co_3O_4 nanostructures towards the sensing of MTX drug.

The practicality of developed PANI assisted Co_3O_4 nanostructures was investigated for two tablets of MTX drug by standard addition and recovery methods and the obtained recovery results are enclosed in Table 2. This study suggests that PANI assisted Co_3O_4 nanostructures have high potential to measure MTX drug precisely. The PANI assisted Co_3O_4 nanostructures were successfully applied to the real blood sample. The blood sample was collected from the Liaquat University of Medical and Health Sciences Jamshoro Sindh Pakistan. The sample preparation was performed by centrifugation for 10 minutes at 12000 rpm. Then plasma was separated out and frozen at -10 ^oC. Afterwards, 100 μL of plasma was added to the 100 μL of methanol, for 30 s and centrifuged for the 10 minutes. After a careful centrifugation supernatant was obtained and used for the electroanalysis and the measured results are given in Table 3. The measured MTX concentration was 0.01μM without the addition of MTX and recovery mhod was also used for the detection of MTX from blood plasma and observed results are satisfactory. The biological matrixes in the blood plasma did not interfere with electrical signal of PANI assisted Co_3O_4 nanostructures, thus the presented protocol has high ability to monitor the MTX drug from real samples.

4. Conclusions

In summary, PANI was used as sacrificing template for the uniform growth of ultra-small Co_3O_4 nanoparticles by hydrothermal method. The ultra-small Co_3O_4 nanoparticles were physically characterized by SEM, EDS, XRD and FTIR techniques. The Co_3O_4 nanoparticles exhibit acceptable oxygen vacancies which played a dynamic role in lifting the electrochemical properties of Co_3O_4 for the oxidation of MTX in BRB buffer of pH 3.5. The PANI assisted Co_3O_4 nanostructures have shown a

significant linear range from 5–75μM for MTX drug with limit of detection of 1.98μM. The PANI assisted Co_3O_4 nanostructures were used practically for the analysis of MTX from real blood plasma sample. The modified electrode is low cost, and very sensitive for the determination of MTX. The proposed strategy involved the PANI as a sacrificing template for the growth of ultra-small Co_3O_4 nanoparticles which can be capitalized into different electrochemical applications.

Declarations

Acknowledgement: The authors thank the British University in Egypt for the support in the SEM imaging through the Nanotechnology Research Centre. The authors extend their sincere appreciation to the Deanship of the Scientific Research at King Saud University for funding this project through Research Group (RG #236)

Conflict of interest: Authors declare no conflict of interest in this research work

References

[1]. Barbosa AI, Fernandes SR, Machado S, Sousa P, Sze OY, Silva EM, Barreiros L, Lima SA, Reis S, Segundo MA (2019) Fast monolith-based chromatographic method for determination of methotrexate in drug delivery studies. Microchemical Journal 148:185-9.

[2]. Rattanarat P, Suea-Ngam A, Ruecha N, Siangproh W, Henry CS, Srisa-Art M, Chailapakul O (2016) Graphene-polyaniline modified electrochemical droplet-based microfluidic sensor for high-throughput determination of 4-aminophenol. Analytica Chimica Acta 925:51-60.

[3]. Rajnics P, Kellner VS, Kellner A, Karadi E, Kollar B, Egyed M (2017) The hematologic t oxicity of methotrexate in patients with autoimmune disorders. J Neoplasm 2:1-6.

[4]. Mutharani B, Ranganathan P, Chen SM, Sireesha P (2019) Ultrasound-induced radicals initiated the formation of inorganic–organic Pr2O3/polystyrene hybrid composite for electro-oxidative determination of chemotherapeutic drug methotrexate. Ultrasonics sonochemistry 56:410-21.

[5]. Meloun M, Ferenčíková Z, Vrána A (2010) The thermodynamic dissociation constants of methotrexate by the nonlinear regression and factor analysis of multiwavelength spectrophotometric pH-titration data. Central European Journal of Chemistry 8:494-507.

[6]. Schnabel A, Gross WL (1994) Low-dose methotrexate in rheumatic diseases—efficacy, side effects, and risk factors for side effects. InSeminars in arthritis and rheumatism 5: 310-327). WB Saunders.

[7]. Gaies E, Jebabli N, Trabelsi S, Salouage I, Charfi R, Lakhal M, Klouz A (2012) Methotrexate side effects: review article J Drug Metab Toxicol 4:1-5.

[8]. Zhou H, Ran G, Masson JF, Wang C, Zhao Y, Song Q (2018) Novel tungsten phosphide embedded nitrogen-doped carbon nanotubes: A portable and renewable monitoring platform for anticancer drug in whole blood. Biosensors and Bioelectronics105:226-35.

[9]. Guichard N, Ogereau M, Falaschi L, Rudaz S, Schappler J, Bonnabry P, Fleury-Souverain S (2018) Determination of 16 antineoplastic drugs by capillary electrophoresis with UV detection: applications in quality control. Electrophoresis 20:2512-20.

[10]. Raichur V, Vemula KD, Bhadri N, Razdan R (2017) Zolendronic acid-conjugated PLGA ultrasmall nanoparticle loaded with methotrexate as a supercarrier for bone-targeted drug delivery. AAPS PharmSciTech 6:2227-39.

[11]. Ensafi AA, Nasr-Esfahani P, Rezaei B (2017) Simultaneous detection of folic acid and methotrexate by an optical sensor based on molecularly imprinted polymers on dual-color CdTe quantum dots. Analytica chimica acta 996:64-73.

[12]. Bouquié R, Grégoire M, Hernando H, Azoulay C, Dailly E, Monteil-Ganière C, Pineau A, Deslandes G, Jolliet P (2016) Evaluation of a Methotrexate Chemiluminescent Microparticle Immunoassay: Comparison to Fluorescence Polarization Immunoassay and Liquid Chromatography–Tandem Mass Spectrometry. American Journal of Clinical Pathology1:119-24.

[13]. Ullah F, Iqbal Z, Raza A, Khan I, Ullah Khan F, Hassan M (2017) Simultaneous determination of methotrexate and metoclopramide in physiological fluids using RP-HPLC with ultra-violet detection; application in evaluation of polymeric nanoparticles. Journal of Liquid Chromatography & Related Technologies 20:1020-30.

[14]. Guo Y, Chen Y, Zhao Q, Shuang S, Dong C (2017) Electrochemical Sensor for Ultrasensitive Determination of Doxorubicin and Methotrexate Based on Cyclodextrin-Graphene Hybrid Nanosheets. Electroanalysis 10:2400-7.

[15]. Manjunatha JG (2017) Surfactant modified carbon nanotube paste electrode for the sensitive determination of mitoxantrone anticancer drug. Journal of Electrochemical Science and Engineering 1:39-49.

[16]. Saleh GA, Askal HF, Refaat IH, Abdel-aal FA (2016) A new electrochemical method for simultaneous determination of acyclovir and methotrexate in pharmaceutical and human plasma samples. Anal. Bioanal. Electrochem 691:e716.

[17]. Wang Y, Liu H, Wang F, Gao Y (2012) Electrochemical oxidation behavior of methotrexate at DNA/SWCNT/Nafion composite film-modified glassy carbon electrode. Journal of Solid State Electrochemistry 10:3227-35.

[18]. Zhu Z, Wu H, Wu S, Huang Z, Zhu Y, Xi L (2013) Determination of methotrexate and folic acid by ion chromatography with electrochemical detection on a functionalized multi-wall carbon nanotube modified electrode. Journal of Chromatography A 1283:62-7.

[19]. Tesfalidet S, Geladi P, Shimizu K, Lindholm-Sethson B (2016) Detection of methotrexate in a flow system using electrochemical impedance spectroscopy and multivariate data analysis. Analytica Chimica Acta 914:1-6.

[20]. Roberts MS, Selvo NS, Roberts JK, Daryani VM, Owens TS, Harstead KE, Gajjar A, Stewart CF (2016) Determination of methotrexate, 7-hydroxymethotrexate, and 2, 4-diamino-N 10-methylpteroic acid by LC–MS/MS in plasma and cerebrospinal fluid and application in a pharmacokinetic analysis of high-dose methotrexate. Journal of liquid chromatography & related technologies 16:745-51.

[21]. Ghadimi H, Nasiri-Tabrizi B, Nia PM, Basirun WJ, Tehrani RM, Lorestani F (2015) Nanocomposites of nitrogen-doped graphene decorated with a palladium silver bimetallic alloy for use as a biosensor for methotrexate detection. RSC advances 120:99555-65.

[22]. Asadian E, Shahrokhian S, Zad AI, Ghorbani-Bidkorbeh F (2017) Glassy carbon electrode modified with 3D graphene–carbon nanotube network for sensitive electrochemical determination of methotrexate. Sensors and Actuators B: Chemical 39:617-27.

[23]. Tesfalidet S, Geladi P, Shimizu K, Lindholm-Sethson B (2016) Detection of methotrexate in a flow system using electrochemical impedance spectroscopy and multivariate data analysis. Analytica Chimica Acta 914:1-6.

[24]. Lima HR, da Silva JS, de Oliveira Farias EA, Teixeira PR, Eiras C, Nunes LC (2018) Electrochemical sensors and biosensors for the analysis of antineoplastic drugs. Biosensors and Bioelectronics 108:27-37.

[25]. Phal S, Lindholm-Sethson B, Geladi P, Shchukarev A, Tesfalidet S (2017) Determination of methotrexate in spiked human blood serum using multi-frequency electrochemical immittance spectroscopy and multivariate data analysis. Analytica chimica acta 987:15-24.

[26]. Janíková-Bandžuchová L, Šelešovská R (2016) Determination of methotrexate at a silver solid amalgam electrode by differential pulse voltammetry. Analytical Letters 1:122-34.

[27]. Solanki PR, Kaushik A, Agrawal VV, Malhotra BD (2011) Nanostructured metal oxide-based biosensors. NPG Asia Materials 1:17-24.

[28]. Mei J, Liao T, Ayoko GA, Bell J, Sun Z (2019) Cobalt oxide-based nanoarchitectures for electrochemical energy applications. Progress in Materials Science 103:596-677.

[29]. Salunkhe RR, Tang J, Kamachi Y, Nakato T, Kim JH, Yamauchi Y (2015) Asymmetric supercapacitors using 3D nanoporous carbon and cobalt oxide electrodes synthesized from a single metal–organic

framework. ACS nano 6:6288-96.

[30]. Wu X, Meng L, Wang Q, Zhang W, Wang Y (2017) A flexible asymmetric fibered-supercapacitor based on unique Co3O4@ PPy core-shell nanorod arrays electrode. Chemical Engineering Journal 327:193-201.

[31]. Tang CH, Yin X, Gong H (2013) Superior performance asymmetric supercapacitors based on a directly grown commercial mass 3D Co3O4@ Ni (OH) 2 core–shell electrode. ACS applied materials & interfaces 21:10574-82.

[32]. Li G, Chen M, Ouyang Y, Yao D, Lu L, Wang L, Xia X, Lei W, Chen SM, Mandler D, Hao Q (2019) Manganese doped Co3O4 mesoporous nanoneedle array for long cycle-stable supercapacitors. Applied Surface Science 469:941-50.

[33]. Wang H, Yang PH, Cai HH, Cai J(2012) Constructions of polyaniline nanofiber-based electrochemical sensor for specific detection of nitrite and sensitive monitoring of ascorbic acid scavenging nitrite. Synthetic metals 162: (3-4):326-31.

[34]. Li R, Chen Z, Li J, Zhang C, Guo Q (2013) Effective synthesis to control the growth of polyaniline nanofibers by interfacial polymerization. Synthetic metals 171:39-44.

[35]. Shen Y, Qin Z, Li T, Zeng F, Chen Y, Liu N (2020) Boosting the supercapacitor performance of polyaniline nanofibers through sulfonic acid assisted oligomer assembly during seeding polymerization process. Electrochimica Acta 356:136841.

[36]. Mafuwe PT, Moyo M, Mugadza T, Shumba M, Nyoni S (2019) Cobalt oxide nanoparticles anchored polyaniline-appended cobalt tetracarboxy phthalocyanine, modified glassy carbon electrode for facile electrocatalysis of amitrole. Journal of Solid State Electrochemistry 1:285-94.

[37]. Houshmand M, Jabbari A, Heli H, Hajjizadeh M, Moosavi-Movahedi AA (2008) Electrocatalytic oxidation of aspirin and acetaminophen on a cobalt hydroxide nanoparticles modified glassy carbon electrode. Journal of Solid State Electrochemistry 9:1117-28.

[38]. Sandhya CP, Baig R, Pillai S, Molji C, Aravind A, Devaki SJ (2019) Polyaniline-cobalt oxide nano shrubs based electrodes for supercapacitors with enhanced electrochemical performance. Electrochimica Acta 324:134876.

[39]. Li T, Zhou Y, Liang B, Jin D, Liu N, Qin Z, Zhu M (2017) One–pot synthesis and electrochemical properties of polyaniline nanofibers through simply tuning acid–base environment of reaction medium. Electrochimica Acta 249:33-42.

[40]. Bhadra J, Al-Thani NJ, Karmakar S, Madi NK (2019) Photo-reduced route of polyaniline nanofiber synthesis with embedded silver nanoparticles. Arabian Journal of Chemistry 8:4848-60.

[41]. Chen S, Liu B, Wang Y, Cheng H, Zhang X, Xu S, Liu H, Liu W, Hu C (2019) Excellent Electrochemical Performances of Intrinsic Polyaniline Nanofibers Fabricated by Electrochemical Deposition. Journal of Wuhan University of Technology-Mater. Sci. Ed. 1:216-22.

[42]. Abdolahi A, Hamzah E, Ibrahim Z, Hashim S (2012) Synthesis of uniform polyaniline nanofibers through interfacial polymerization. Materials 8:1487-94.

[43]. Liu Y, Zhu G, Ge B, Zhou H, Yuan A, Shen X (2012) Concave Co 3 O 4 octahedral mesocrystal: polymer-mediated synthesis and sensing properties. CrystEngComm 19:6264-70.

[44]. He T, Chen D, Jiao X, Xu Y, Gu Y (2004) Surfactant-assisted solvothermal synthesis of Co3O4 hollow spheres with oriented-aggregation nanostructures and tunable particle size. Langmuir 19:8404-8.

[45]. Xia XH, Tu JP, Mai YJ, Wang XL, Gu CD, Zhao XB (2011) Self-supported hydrothermal synthesized hollow Co3O4 nanowire arrays with high supercapacitor capacitance. Journal of Materials Chemistry 25:9319-25.

[46]. Vijayakumar S, Ponnalagi AK, Nagamuthu S, Muralidharan G (2013) Microwave assisted synthesis of Co3O4 nanoparticles for high-performance supercapacitors. Electrochimica Acta 106:500-5.

[47]. Shambharkar BH, Umare SS (2010) Production and characterization of polyaniline/Co3O4 nanocomposite as a cathode of Zn–polyaniline battery. Materials Science and Engineering: B 2:120-8.

[48]. Boomi P, Prabu HG, Manisankar P, Ravikumar S (2014) Study on antibacterial activity of chemically synthesized PANI-Ag-Au nanocomposite. Applied Surface Science 300:66-72.

[49]. Zheng W, Angelopoulos M, Epstein AJ, MacDiarmid AG (1997) Experimental evidence for hydrogen bonding in polyaniline: mechanism of aggregate formation and dependency on oxidation state. Macromolecules 10:2953-5.

[50]. Xu F, Ma L, Huo Q, Gan M, Tang J (2015) Microwave absorbing properties and structural design of microwave absorbers based on polyaniline and polyaniline/magnetite nanocomposite. Journal of Magnetism and Magnetic Materials 374:311-6.

[51]. Erdemi H, Baykal A, Karaoğlu E, Toprak MS (2012) Synthesis and conductivity studies of piperidine-4-carboxylic acid functionalized Fe3O4 nanoparticles. Materials Research Bulletin 9:2193-9.

[52]. Nosrati H, Salehiabar M, Davaran S, Danafar H, Manjili HK (2018) Methotrexate-conjugated L-lysine coated iron oxide magnetic nanoparticles for inhibition of MCF-7 breast cancer cells. Drug development and industrial pharmacy 6:886-94.

[53]. 49. Amin. S, Tahira. A, Solangi. A.R, Mazzaro. R, Ibupoto.Z.H, Fatima. A, Vomiero. A, (2020) Functional Nickel Oxide Nanostructures for Ethanol Oxidation in Alkaline Media. Electroanalysis 32: 1052-1059

Tables

Table I. Interference Studies

Interfering reagent	Concentration (μM)	Signal Increase
Paclitaxel	60	2.54
Mitoxantrone	60	-3.32
Glucose	60	0.2
Sucrose	60	-2.9
Urea	60	1.3
Chloride	60	2.65

Table II: Recovery results

Tablet Number	Added μM	Found μM	% Recovery	RSD (%)
1	30	31.01	103.36	3.23
	40	39.62	99.05	0.98
	50	49.99	99.98	1.34
2	30	30.09	100.3	1.45
	40	40.07	100.7	0.59
	50	50.07	100.7	1.59

Table III: Real sample analysis

Blood Plasma	Added μM	Found μM	% Recovery	RSD (%)
1	00	0.01	103.36	1.23
	30	29.02	96.73	3.98
	35	37.06	105.88	4.34

Figures

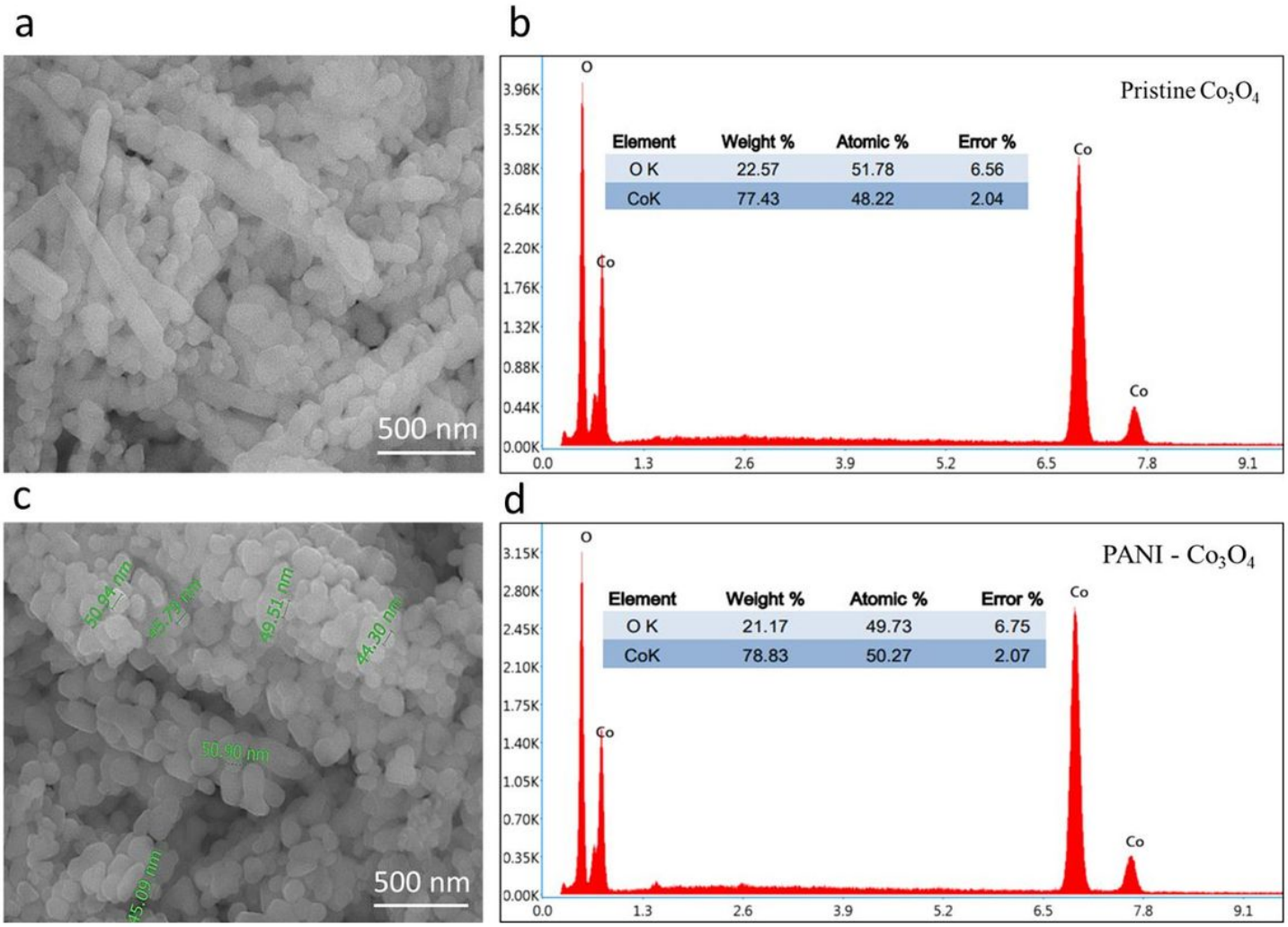

Figure 1

Typical SEM images a. pristine Co3O4, b. EDS spectrum of pristine Co3O4, c. PANI assisted Co3O4 nanoparticles, d. EDS spectrum of PANI assisted Co3O4

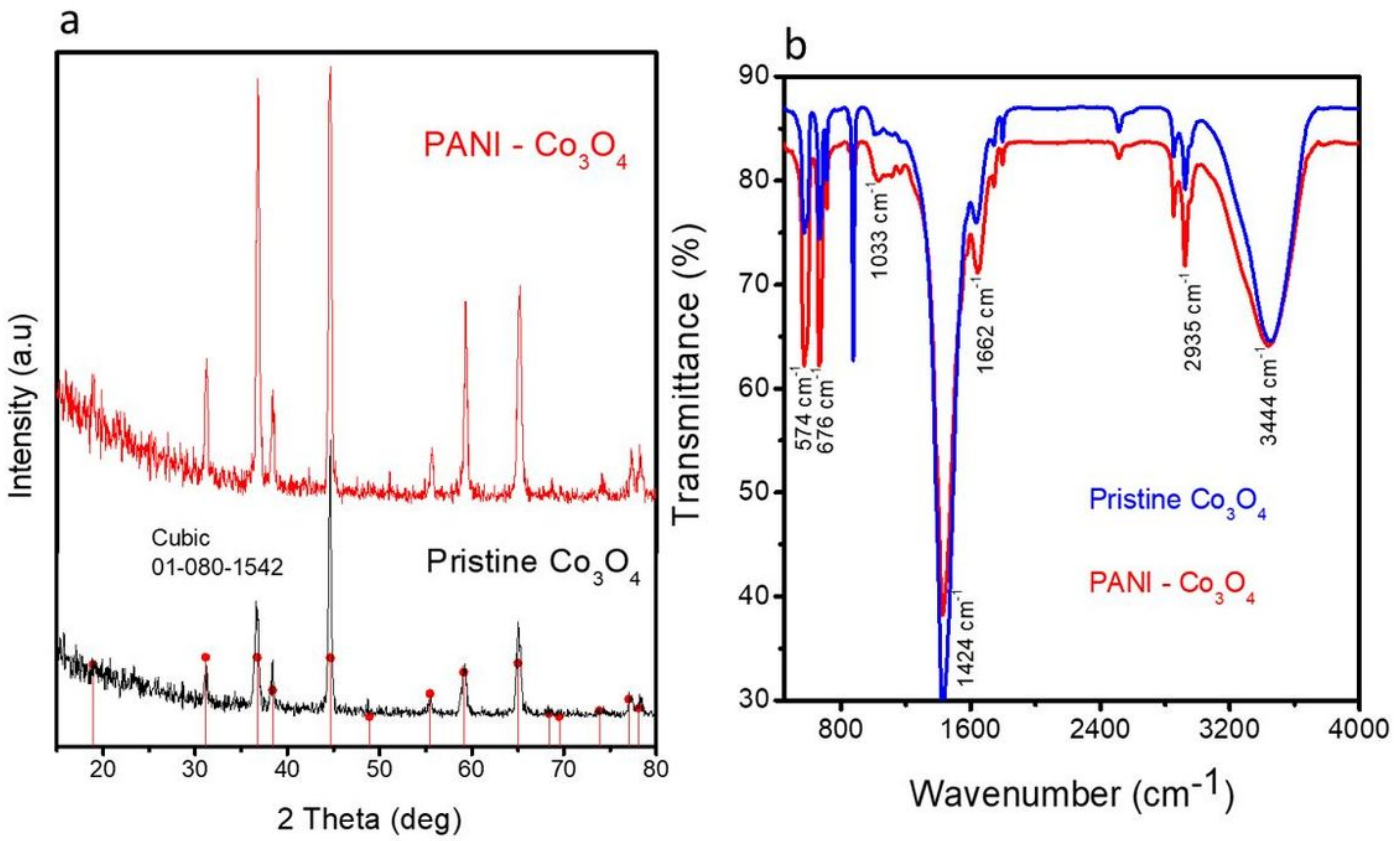

Figure 2

a. XRD reflection of pristine Co3O4 and PANI assisted Co3O4 nanoparticles, b. FTIR spectra of pristine Co3O4 and PANI assisted Co3O4 nanoparticles

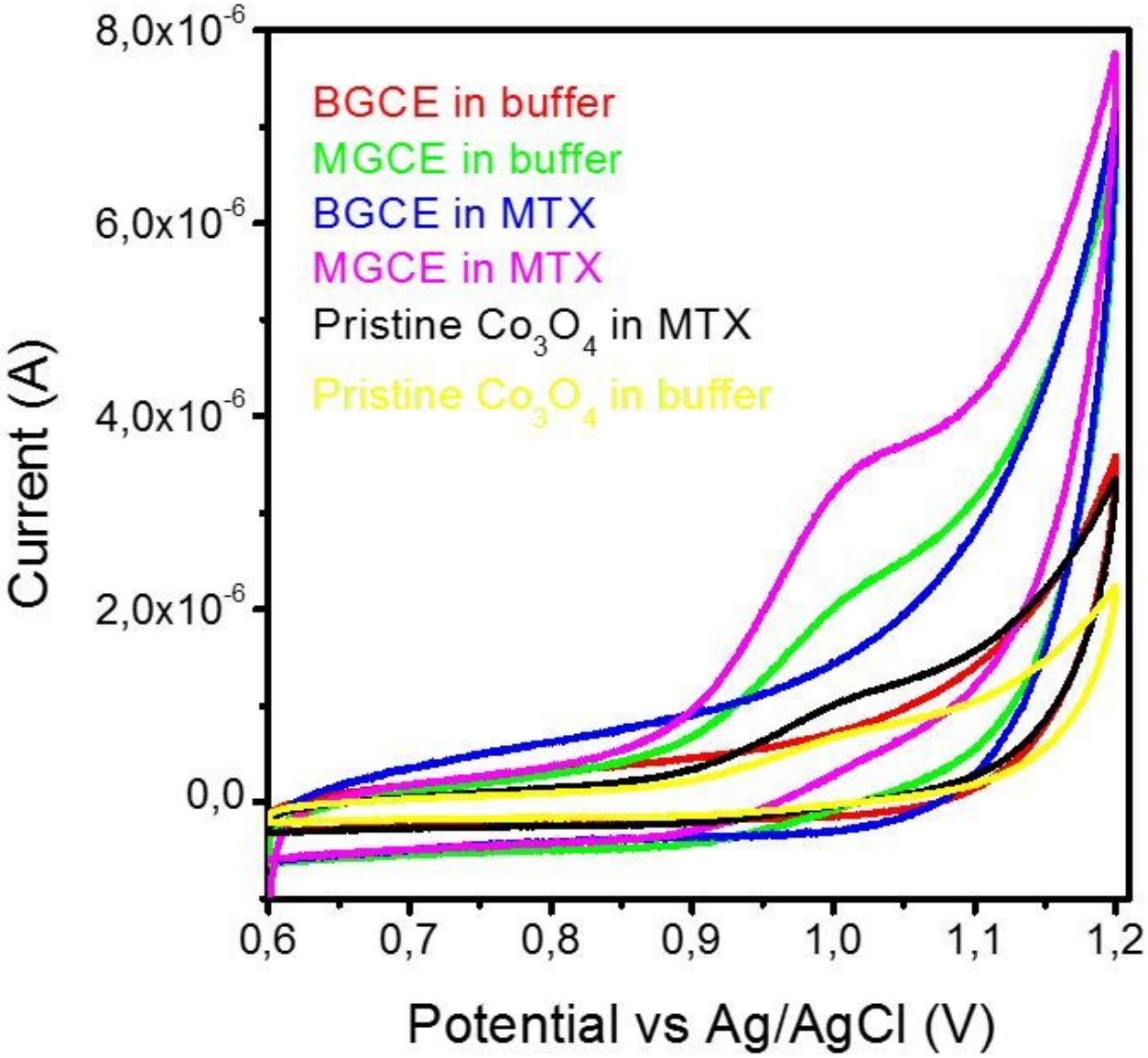

Figure 3

CV curves of bare GCE, pristine Co3O4 and PANI assisted Co3O4 nanoparticles in 0.01M BRB buffer of pH 3.5, and pristine Co3O4 and PANI assisted Co3O4 nanoparticles in 20µM MTX concentration prepared in 0.01M BRB buffer of pH 3.5 at a scan rate of 60 mV/s

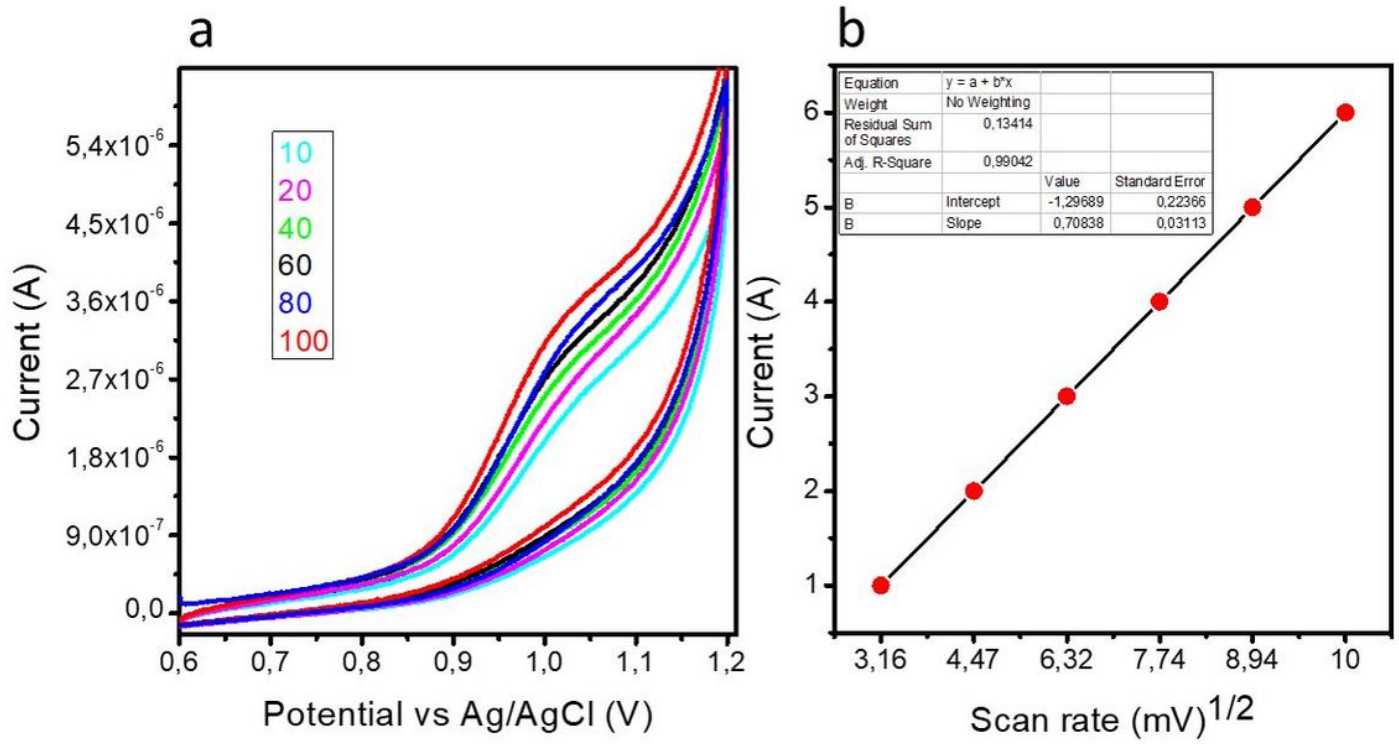

Figure 4

a. CV curves of PANI assisted Co3O4 nanoparticles at various scan rates in 20µM MTX concentration, b. linear plot of peak current versus square of scan rate

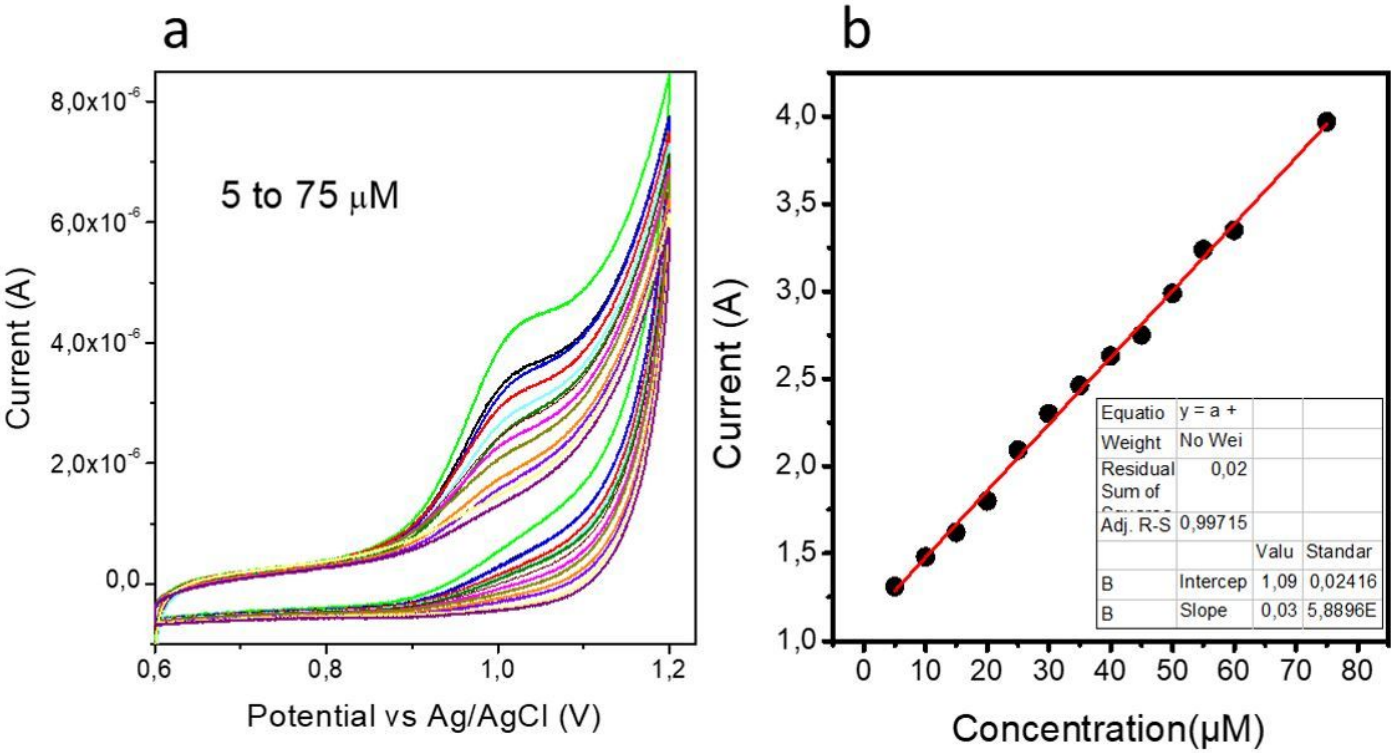

Figure 5

a. CV curves of PANI assisted Co3O4 nanoparticles in various concentrations of MTX ranging from 5-75 µM prepared in 0.01M BRB buffer solution of pH 3.5 at a scan rate of 60 mV/s, b. Linear fitting of peak current versus various concentrations of MTX drug

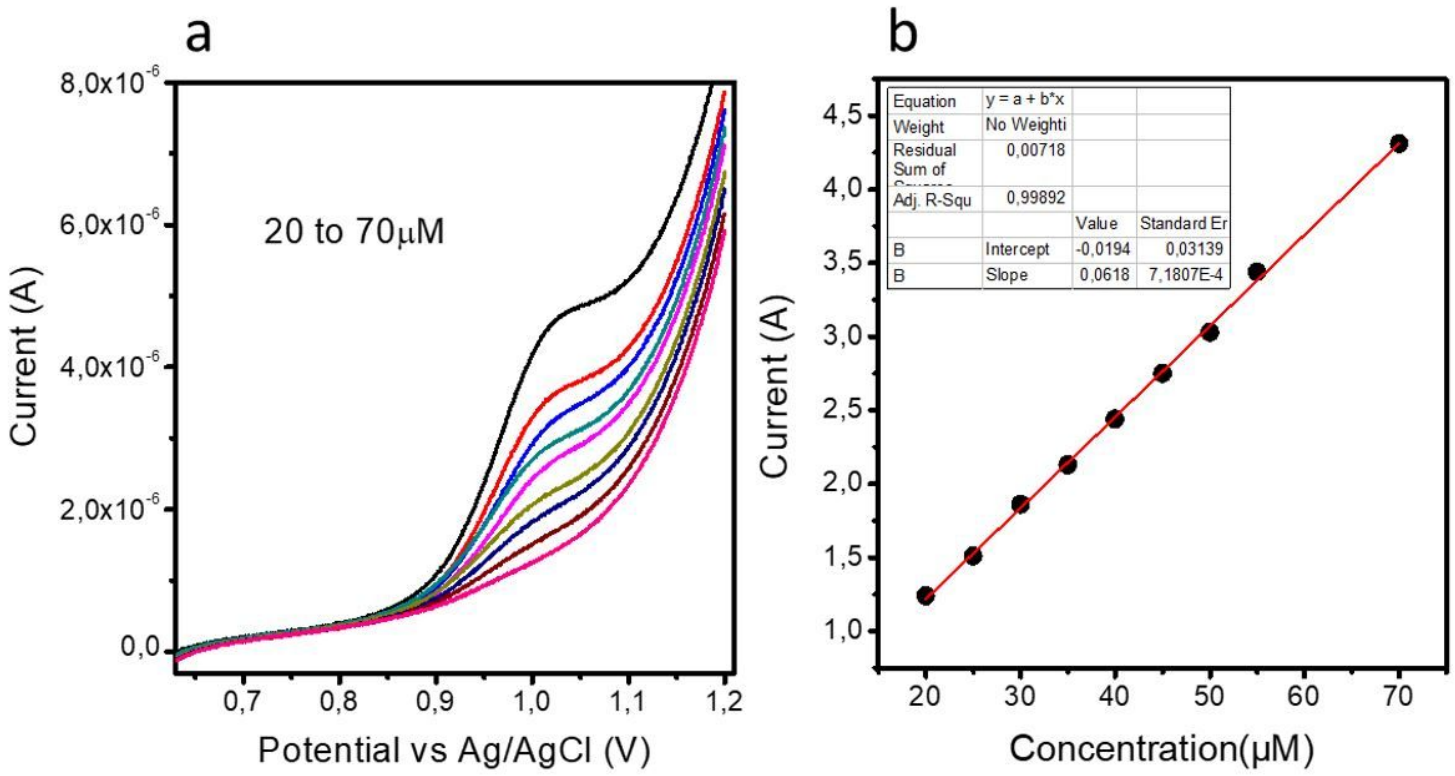

Figure 6

a. LSV curves of PANI assisted Co3O4 nanoparticles in different concentrations of MTX from 20-70µM at a scan rate of 10 mV/s, b. Linear plot of peak current against different concentrations of MTX drug

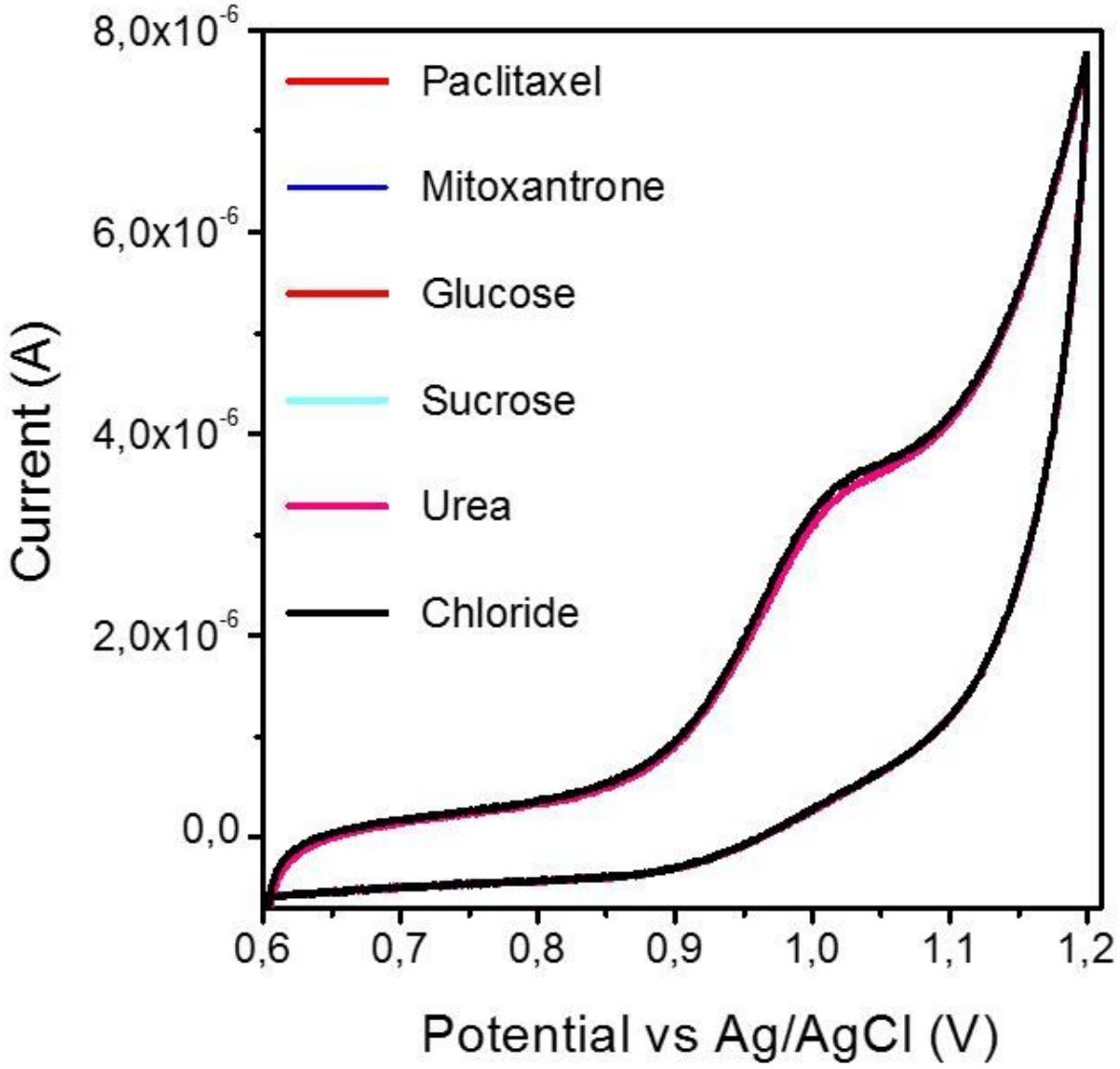

Figure 7

CV curves of PANI assisted Co3O4 nanoparticles in 20μM MTX concentration prepared in 0.01M BRB buffer solution of pH 3.5 and various competing substances at a scan rate of 60 mV/s